Int. J. Solids Structures, 1973, Vol. 9, pp. 395 to 414. Pergamon Press. Printed in Great Britain

A CONTINUUM MIXTURE THEORY OF WAVE PROPAGATION IN LAMINATED AND FIBER REINFORCED COMPOSITES

G. A. HEGEMIER

Department of Applied Mechanics and Engineering Science, University of California, San Diego, La Jolla, California

and

G. A. GURTMAN and ADNAN H. NAYFEH

Systems, Science and Software, La Jolla, California

Abstract—A binary mixture theory is developed for wave guide-type propagation in laminated and undirectional fibrous composites. In particular, a rational construction of both mixture interaction and constitutive relations is given. The resulting theory contains microstructure.

The domain of validity of the mixture theory is determined by comparison of the phase velocity spectrum with exact and/or experimental results. The utility of the model is demonstrated for both laminated and fibrous composites by correlating theoretical and experimental transient pulse data on boron–carbon phenolic and Thornel–carbon phenolic laminates, and uni-directional fibrous quartz phenolic.

1. INTRODUCTION

IN RECENT years several continuum theories have been proposed as models of the elastostatics or elastodynamics of composite materials.

The so-called "effective modulus" theories, such as those proposed by Postma [1] and White and Angona [2] replace the actual composite by a homogeneous, generally anisotropic medium whose material constants are a geometrically weighted average of the properties of the constituents. While yielding satisfactory results for certain geometries under static loads, such an approach exhibits serious deficiences for virtually all geometries when applied to wave propagation. Specifically, effective modulus theories are incapable of reproducing the dispersion and attenuation observed in composites. Such behavior is a result of the microstructure of the particular composite; consequently, any continuum theory designed to account for it must, in some fashion, reflect the effect of microstructure.

One model satisfying this criteria is the so-called "effective stiffness" theory proposed by Achenbach, Herrmann and Sun [3–5]. Here the actual composite is transformed into a homogeneous higher order continuum with microstructure.

Another approach is that taken by Lempriere [6] and Bedford and Stern [7]. These investigators propose mixture theories as models of the elastodynamics of composites. The composite constituents are superimposed in space and allowed to undergo individual deformations. The microstructure of the actual composite is then simulated by specifying the interactions between the constituents. For the case of a one-dimensional (on the average)

wave propagating in a two-component mixture, Lempriere hypothesizes the nature of these interactions as being dependent upon either the displacement or velocity difference in the two constituents. For laminates running in the direction of propagation, Bedford and Stern offer an analytical procedure to determine these interactions, based upon a quasi-static analysis of the composite.

In this paper we present an alternate analytical procedure for the development of binary mixture theories modeling wave propagation in laminated and uni-directional fibrous composites. We consider the case where propagation is parallel to both laminates and fibers. In particular, a rational construction of the mixture interaction and constitutive relations is given. The resulting theory contains microstructure, i.e. information on the distribution of displacements and stresses within individual constituents.

The theoretical approach is such that models of arbitrary orders of accuracy can be determined. In this paper, however, attention is focused on the development of a first order theory whose simplicity will, it is hoped, lead to maximum utility.

The domain of validity of the first order mixture theory is investigated by comparison of the phase velocity spectrum with exact and/or experimental results. The utility of the first order dispersive theory is demonstrated for both laminated and fibrous composites by correlating theoretical and experimental transient pulse data on boron–carbon phenolic and Thornel–carbon phenolic laminates, and uni-directional fibrous quartz phenolic.

2. ANALYSIS AND RESULTS FOR LAMINATED COMPOSITES

Formulation

Consider a periodic array of two linearly elastic, isotropic, and homogeneous laminates, bonded at their interfaces. A state of plane strain will be assumed in the z-direction, as well as wave motion yielding symmetric u_x and antisymmetric u_y distributions with respect to the y-coordinate within each laminate, where u_x and u_y denote displacements in the x- and y-directions, respectively. Consequently, averaged motion of laminates exists only in the x-direction, and it is sufficient to consider a typical bi-laminate as illustrated in Fig. 1.

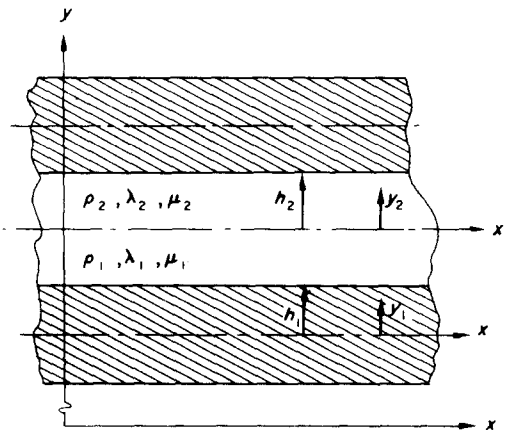

FIG. 1. Laminated composite geometry and coordinate system.

The basic equations for the laminates are:

(i) Equations of motion:

$$\partial_x \overset{(\alpha)}{\sigma}_{xx} + \partial_{y_\alpha} \overset{(\alpha)}{\sigma}_{xy} = \rho_\alpha \partial_t^2 \overset{(\alpha)}{u}_x, \tag{2.1a}$$

$$\partial_{y_\alpha} \overset{(\alpha)}{\sigma}_{yy} + \partial_x \overset{(\alpha)}{\sigma}_{xy} = \rho_\alpha \partial_t^2 \overset{(\alpha)}{u}_y, \tag{2.1b}$$

(ii) Constitutive relations:

$$\overset{(\alpha)}{\sigma}_{xx} = (\lambda + 2\mu)_\alpha \partial_x \overset{(\alpha)}{u}_x + \lambda_\alpha \partial_{y_\alpha} \overset{(\alpha)}{u}_y, \tag{2.2a}$$

$$\overset{(\alpha)}{\sigma}_{yy} = (\lambda + 2\mu)_\alpha \partial_{y_\alpha} \overset{(\alpha)}{u}_y + \lambda_\alpha \partial_x \overset{(\alpha)}{u}_x, \tag{2.2b}$$

$$\overset{(\alpha)}{\sigma}_{xy} = \mu_\alpha (\partial_{y_\alpha} \overset{(\alpha)}{u}_x + \partial_x \overset{(\alpha)}{u}_y), \tag{2.2c}$$

where

$$\partial_x^n(\ ) \equiv \partial^n(\ )/\partial x^n, \qquad \partial_t^n(\ ) \equiv \partial^n(\ )/\partial t^n,$$

σ_{xx}, σ_{xy}, etc. are components of the stress tensor, ρ_α is the mass density of material, α, t denotes time, y_α is a local coordinate in the y-direction with origin at the midplane of the α-constituent, and the superscript or subscript $\alpha (= 1, 2)$ refers to the α-constituent.

In addition to equations (2.1) and (2.2), the complete specification of motion requires

(iii) Symmetry conditions:

$$\overset{(\alpha)}{u}_y = 0, \qquad \overset{(\alpha)}{\sigma}_{xy} = 0 \qquad \text{on } y_\alpha = 0, \tag{2.3}$$

(iv) Interface conditions:

$$\overset{(1)}{u}_y = \overset{(2)}{u}_y, \qquad \overset{(1)}{u}_x = \overset{(2)}{u}_x, \qquad \overset{(1)}{\sigma}_{xy} = \overset{(2)}{\sigma}_{xy}, \qquad \overset{(1)}{\sigma}_{yy} = \overset{(2)}{\sigma}_{yy} \tag{2.4}$$

on $y_1 = h_1, y_2 = -h_2$.

(v) Initial conditions at $t = 0$, and appropriate boundary data at $x = 0, L$, where $x \in [0, L]$.

Mixture equations of motion

If (2.1a) is integrated with respect to y_α from 0 to h_α, and averaged stresses and displacements are defined according to

$$\overset{(\alpha a)}{(\ )} \equiv \frac{1}{h_\alpha} \int_0^{h_\alpha} \overset{(\alpha)}{(\ )}\, dy, \tag{2.5}$$

where h_α denotes the half thickness of laminates of material α, then (2.1a) can be written as

$$h_\alpha \partial_x \overset{(\alpha a)}{\sigma}_{xx} - h_\alpha \rho_\alpha \partial_t^2 \overset{(\alpha a)}{u}_x = -\overset{(\alpha)}{\sigma}_{xy}(x, h_\alpha, t). \tag{2.6}$$

Since $\overset{(\alpha)}{\sigma}_{xy}$ must be continuous across laminate interfaces (see 2.4) and is asymmetric in y_α, one deduces that

$$-\overset{(1)}{\sigma}_{xy}(x, h_1, t) = \overset{(2)}{\sigma}_{xy}(x, h_2, t) \equiv \sigma^*_{xy}(x, t). \tag{2.7}$$

With the aid of (2.7), equations (2.6) can be placed in a standard binary mixture form by introducing the following "partial" stresses and densities:

$$\overset{(\alpha p)}{\sigma_{xx}} \equiv n_\alpha \overset{(\alpha a)}{\sigma_{xx}}, \qquad \overset{(p)}{\rho_\alpha} \equiv n_\alpha \rho_\alpha, \tag{2.8}$$

where

$$n_\alpha \equiv h_\alpha/(h_1+h_2) \tag{2.9}$$

is a volume fraction of the α-constituent. Utilizing (2.7) and (2.8), the momentum equations (2.6) become

$$\partial_x \overset{(1p)}{\sigma_{xx}} - \overset{(p)}{\rho_1} \partial_t^2 \overset{(1a)}{u_x} = P, \tag{2.10a}$$

$$\partial_x \overset{(2p)}{\sigma_{xx}} - \overset{(p)}{\rho_2} \partial_t^2 \overset{(2a)}{u_x} = -P, \tag{2.10b}$$

where

$$P = \sigma^*_{xy}/(h_1+h_2) \tag{2.11}$$

is an "interaction" term reflecting momentum transfer from one constituent to another via shear interaction across laminate interfaces.

To this point the analysis essentially parallels that of Bedford and Stern [7]. We now propose an alternate procedure for the analytical determination of the interaction term P and the mixture constitutive relations.

Expansions and recurrence relations

The procedure commences by assuming a power-series expansion for stresses and displacements about the midplane of each laminate. Thus we have

$$\overset{(\alpha)}{g}(x, y_\alpha, t) = \overset{(\alpha)}{g_{(0)}}(x,t) + \overset{(\alpha)}{g_{(1)}}(x,t) y_\alpha + \ldots \overset{(\alpha)}{g_{(n)}}(x,t) y_\alpha^n/n! + \ldots, \tag{2.12}$$

where $\overset{(\alpha)}{g}$ represents stress or displacement in the α-constituent. We note that the series (2.12) need not be convergent, but only asymptotic in a parameter ε as $\varepsilon \to 0$, where ε represents the ratio of typical micro-to-macro-dimensions of the composite. For complete details concerning this point, the reader is referred to [8].

Substituting (2.12) into equation (2.1) through (2.2), and equating terms of similar order of y_α, one obtains the following differential-recurrence relation for the coefficients of the expansion (2.12):

$$\partial_x \overset{(\alpha)}{\sigma_{xx(n)}} + \overset{(\alpha)}{\sigma_{xy(n+1)}} = \rho_\alpha \partial_t^2 \overset{(\alpha)}{u_{x(n)}}, \tag{2.13a}$$

$$\overset{(\alpha)}{\sigma_{yy(n+1)}} + \partial_x \overset{(\alpha)}{\sigma_{xy(n)}} = \rho_\alpha \partial_t^2 \overset{(\alpha)}{u_{y(n)}}, \tag{2.13b}$$

$$\overset{(\alpha)}{\sigma_{xx(n)}} = (\lambda+2\mu)_\alpha \partial_x \overset{(\alpha)}{u_{x(n)}} + \lambda_\alpha \overset{(\alpha)}{u_{y(n+1)}}, \tag{2.14a}$$

$$\overset{(\alpha)}{\sigma_{yy(n)}} = (\lambda+2\mu)_\alpha \overset{(\alpha)}{u_{y(n+1)}} + \lambda_\alpha \partial_x \overset{(\alpha)}{u_{x(n)}}, \tag{2.14b}$$

$$\overset{(\alpha)}{\sigma_{xy(n)}} = \mu_\alpha (\overset{(\alpha)}{u_{x(n+1)}} + \partial_x \overset{(\alpha)}{u_{y(n)}}). \tag{2.14c}$$

Equations (2.13a), (2.14a, b) apply for $n = 0, 2, 4, \ldots$, whereas (2.13b), (2.14c) are valid for $n = 1, 3, 5, \ldots$. It is noted that

$$\overset{(\alpha)}{\sigma}_{xy(n)} = \overset{(\alpha)}{u}_{y(n)} = 0 \quad \text{for } n = 0, 2, 4, \ldots,$$
$$\overset{(\alpha)}{\sigma}_{xx(n)} = \overset{(\alpha)}{\sigma}_{yy(n)} = \overset{(\alpha)}{u}_{x(n)} = 0 \quad \text{for } n = 1, 3, 5, \ldots. \tag{2.14d}$$

Conditions (2.14d) follow from symmetry or asymmetry of appropriate stresses and displacements.

Using the differential-recurrence relations (2.13–14), all stresses and displacements may now be written in terms of the dependent variables of the mixture momentum equations (2.10) as follows:

$$\overset{(\alpha)}{g}(x, y_\alpha, t) = \left(\sum_n \overset{(\alpha)}{\mathscr{L}}_{(n)}(x, t) y^n/n!\right)^{(\alpha a)} \overset{(\alpha a)}{u}_x + \left(\sum_n \overset{(\alpha)}{\mathscr{M}}_{(n)}(x, t) y^n/n!\right)^{(\alpha p)} \overset{(\alpha p)}{\sigma}_{xx}, \tag{2.15}$$

where $\overset{(\alpha)}{\mathscr{L}}_{(n)}$ and $\overset{(\alpha)}{\mathscr{M}}_{(n)}$ are linear differential operators with respect to x and t.

Since the objective of the present paper is a rational development of a first order mixture theory, it will be necessary to derive only the first term or two of the foregoing operators. Details concerning the complete determination of all operators and resulting higher order theories can be found in [8].

Mixture constitutive relations

If equations (2.2a) and (2.2b) are averaged according to (2.5) and continuity of $\overset{(\alpha)}{u}_y$ across laminate interfaces is invoked, the result is

$$n_1\left[\frac{\overset{(1a)}{\sigma}_{xx}}{\lambda_1} - \frac{E_1}{\lambda_1}\partial_x \overset{(1a)}{u}_x\right] = -S, \tag{2.16a}$$

$$n_2\left[\frac{\overset{(2a)}{\sigma}_{xx}}{\lambda_2} - \frac{E_2}{\lambda_2}\partial_x \overset{(2a)}{u}_x\right] = S, \tag{2.16b}$$

$$n_1\left[\frac{\overset{(1a)}{\sigma}_{yy}}{E_1} - \frac{\lambda_1}{E_1}\partial_x \overset{(1a)}{u}_x\right] = -S, \tag{2.16c}$$

$$n_2\left[\frac{\overset{(2a)}{\sigma}_{yy}}{E_2} - \frac{\lambda_2}{E_2}\partial_x \overset{(2a)}{u}_x\right] = S, \tag{2.16d}$$

where

$$S \equiv u_y^*(x, t)/(h_1 + h_2), \tag{2.17a}$$

$$u_y^* \equiv \overset{(2)}{u}_y(x, h_2, t) = \overset{(1)}{u}_y(x_1 - h_1, t) = -\overset{(1)}{u}_y(x, h_1, t), \tag{2.17b}$$

$$E_\alpha \equiv (\lambda + 2\mu)_\alpha. \tag{2.17c}$$

Now, let the characteristic dominant signal wavelength of wave motion be l, and the typical composite microdimension be h_1+h_2. Further, consider the nondimensional variables:

$$\xi = x/l, \qquad \zeta_\alpha = y_\alpha/(h_1+h_2),$$
$$\tau = tc_0/l, \qquad \varepsilon = (h_1+h_2)/l, \tag{2.18a}$$

where c_0 denotes a representative "mixture" velocity (to be defined later). Then if $x \in (0, l)$, $t \in (0, l/c_0)$, we have $\xi \in (0, 1)$, $\tau \in (0, 1)$; i.e. the typical macrodimension is now $O(1)$ whereas the typical microdimension is $O(\varepsilon)$.

With the aid of the recurrence relations (2.13–14), the nondimensional variables (2.18a), and the assumption that l may be selected such that

$$\partial_\xi(\ ) = O(1), \qquad \partial_\tau(\ ) = O(1),$$

where ( ) represents

$$\overset{(\alpha a)}{u_x} \quad \text{or} \quad \overset{(\alpha p)}{\sigma_{xx}},$$

the stress continuity condition

$$\overset{(1)}{\sigma_{yy}}(x, h_1, l) = \overset{(2)}{\sigma_{yy}}(x, -h_2, l)$$

can be written

$$[1+O(\varepsilon^2)]\overset{(1a)}{\sigma_{yy}} = [1+O(\varepsilon^2)]\overset{(2a)}{\sigma_{yy}}. \tag{2.18b}$$

In what follows it will be assumed that $\varepsilon \ll 1$. We shall neglect the $O(\varepsilon^2)$ terms here and adopt the approximation

$$\overset{(1a)}{\sigma_{yy}} \approx \overset{(2a)}{\sigma_{yy}} \tag{2.18c}$$

whereupon (2.16c, d) yield

$$S = \frac{1}{E}(\lambda_1\partial_x\overset{(1a)}{u} - \lambda_2\partial_x\overset{(2a)}{u}), \tag{2.19a}$$

where

$$E \equiv \frac{E_1}{n_1} + \frac{E_2}{n_2}. \tag{2.19b}$$

Substituting (2.19) into (2.16a, b) furnishes

$$\overset{(1p)}{\sigma_{xx}} \simeq c_{11}\partial_x\overset{(1a)}{u_x} + c_{12}\partial_x\overset{(2a)}{u_x}, \tag{2.20a}$$

$$\overset{(2p)}{\sigma_{xx}} \simeq c_{12}\partial_x\overset{(1a)}{u_x} + c_{22}\partial_x\overset{(2a)}{u_x}, \tag{2.20b}$$

where

$$c_{\alpha\alpha} = \left(n_\alpha E_\alpha - \frac{\lambda_\alpha^2}{E}\right), \qquad c_{\alpha\beta} = \frac{\lambda_\alpha\lambda_\beta}{E}, \tag{2.21}$$

$$(\alpha, \beta = 1, 2, ; \alpha \neq \beta).$$

Equations (2.20) are the mixture constitutive equations, subject to the approximation (2.18c). A higher order theory can be generated by relaxing (2.18c) and employing the differential-recurrence relations (2.13) and (2.14). In such a case the coefficients $c_{\alpha\beta}$ would become differential operators in x and t. For most engineering applications, however, the present "first order" theory should be adequate.

Interaction term P

To solve for P we multiply (2.2c) by y_α and integrate as follows:

$$\frac{1}{h_\alpha}\int_0^{h_\alpha} y_\alpha\left[\partial_{y_\alpha}\overset{(\alpha)}{u}_x+\partial_x\overset{(\alpha)}{u}_y-\frac{\overset{(\alpha)}{\sigma}_{xy}}{\mu_\alpha}\right]\mathrm{d}y=0. \tag{2.22}$$

Upon expanding $\partial_x\overset{(\alpha)}{u}_y-\overset{(\alpha)}{\sigma}_{xy}/\mu_\alpha$ in powers of y_α according to (2.12–2.15), and subsequently integrating by parts, we find

$$\overset{(\alpha)}{u}_x(x,h_\alpha,t)-\overset{(\alpha a)}{u}_x+\frac{h_\alpha^2}{3}\left(\partial_x\overset{(\alpha)}{u}_{y(1)}-\frac{1}{\mu_\alpha}\overset{(a)}{\sigma}_{xy(1)}\right)+\ldots=0. \tag{2.23a}$$

With use of the expansion (2.12), and the recurrence relations (2.13–2.14), the higher order terms in (2.23a) may be grouped in the form

$$\overset{(\alpha)}{u}_x(x,h_\alpha,t)-\overset{(\alpha a)}{u}_x+\frac{h_\alpha}{3}\left[(1+\overset{(\alpha)}{\eta}_1\varepsilon^2+\ldots)\partial_x\overset{(\alpha)}{u}_y(x,h_\alpha,t)-\frac{1}{\mu_\alpha}(1+\overset{(\alpha)}{\eta}_2\varepsilon^2+\ldots)\overset{(\alpha)}{\sigma}_{xy}(x,h_\alpha,t)\right]=0, \tag{2.23b}$$

where $\overset{(\alpha)}{\eta}_\beta$ are second order differential operators in ξ and τ. As before, since $\varepsilon\ll 1$, we shall neglect all $O(\varepsilon^2)$ terms in (2.23b). Under this approximation, and using (2.7), (2.17b), we find

$$\begin{aligned}\overset{(1)}{u}_x(x,h_1,t)-\overset{(1a)}{u}_x+\frac{h_1}{3}\left(\frac{1}{\mu_1}\sigma^*_{xy}-\partial_x u^*_y\right)&=0,\\ \overset{(2)}{u}_x(x,h_2,t)-\overset{(2a)}{u}_x+\frac{h_2}{3}\left(\partial_x u^*_y-\frac{1}{\mu_2}\sigma^*_{xy}\right)&=0.\end{aligned} \tag{2.24}$$

Since

$$\overset{(1)}{u}_x(x,h_1,t)=\overset{(1)}{u}_x(x,-h_1,t)=\overset{(2)}{u}_x(x,h_2,t). \tag{2.25}$$

Equations (2.24) can be solved for σ^*_{xy} as follows:

$$\sigma^*_{xy}=\frac{3\mu_1\mu_2}{h_1\mu_2+h_2\mu_1}\left\{\left[1+\frac{\lambda_1\varepsilon^2}{3E}\partial_\xi^2\right]\overset{(1a)}{u}_x-\left[1+\frac{\lambda_2\varepsilon^2}{3E}\partial_\xi^2\right]\overset{(2a)}{u}_x\right\}. \tag{2.26a}$$

If $\varepsilon^2\ll 1$, it is reasonable to neglect $O(\varepsilon^2)$ terms in (2.26a). Under this approximation, the interaction term $P=\sigma^*_{xy}/(h_1+h_2)$ takes the form

$$P\simeq\frac{K}{(h_1+h_2)^2}(\overset{(1a)}{u}_x-\overset{(2a)}{u}_x), \tag{2.26b}$$

where

$$K = 3\mu_1\mu_2/(\mu_1 n_2 + \mu_2 n_1). \tag{2.26c}$$

It is noted that (2.26b) is identical to that obtained by Bedford and Stern [7].

Phase velocity spectrum

In an effort to ascertain the domain of validity of the foregoing continuum model, we now investigate the phase velocity spectrum. For this purpose, equation (2.10), (2.20) and (2.26b) may be reduced to the following global equation for both stresses and displacements:

$$\left[-\frac{\gamma}{(h_1+h_2)^2}(c_0^2\partial_x^2 - \partial_t^2) + (c_1^2c_2^2 - c_3^4)\partial_x^4 - (c_1^2+c_2^2)\partial_x^2\partial_t^2 + \partial_t^4\right]\Phi = 0, \tag{2.27}$$

where

$$c_0^2 \equiv (c_{11}+c_{22}+2c_{12})/\rho, \qquad c_1^2 \equiv c_{11}/\overset{(p)}{\rho}_1, \qquad c_2^2 \equiv c_{22}/\overset{(p)}{\rho}_2,$$
$$c_3^4 \equiv c_{12}^2/\overset{(p)}{\rho}_1\overset{(p)}{\rho}_2, \qquad \gamma \equiv K[\rho/\overset{(p)}{\rho}_1\overset{(p)}{\rho}_2], \tag{2.28}$$

and ρ is a "mixture density" defined by $\rho \equiv \overset{(p)}{\rho}_1 + \overset{(p)}{\rho}_2$. The function Φ in (2.27) represents either stress or displacement of constituent 1 or 2.

The phase velocity spectrum of (2.27) is obtained by seeking a solution of the form

$$\Phi = \Phi^* e^{i(kx-\omega t)}, \tag{2.29}$$

where k, ω, Φ^* denote wave number, circular frequency, and wave amplitude, respectively. Substitution of (2.29) into (2.27) yields the following relation between the phase velocity $c_p \equiv \omega/\mathrm{Re}(K)$ and frequency:

$$\omega = \left[\frac{\gamma(c_p^2 - c_0^2)c_p^2}{(c_-^2 - c_p^2)(c_+^2 - c_p^2)}\right]^{\frac{1}{2}}, \tag{2.30a}$$

where

$$c_\pm^2 = \frac{c_1^2 + c_2^2 \pm \sqrt{[(c_1^2 - c_2^2)^2 + 4c_3^4]}}{2}. \tag{2.30b}$$

Equation (2.30) is similar in form to the dispersion relations derived by Lempriere [6].

The basic character of (2.30) is worthy of mention. We note that if the material properties of both constituents are equal, $c_p = c_0$ satisfies (2.30a), and implies the medium is non-dispersive.

In the general case the character of the solution in four basic regions of the $c_p - \omega$ plane is as follows:

(I) $0 \le c_p \le c_-$ no real solution;
(II) $c_- \le c_p \le c_0$ real solution, $\mathscr{L}_{\omega\to 0}\, c_p = c_0$, $\mathscr{L}_{\omega\to\infty}\, c_p = c_-$;
(III) $c_0 \le c_p \le c_+$ no real solution;
(IV) $c_p \ge c_+$ real solution, $\mathscr{L}_{\omega\to\infty}\, c_p = c_+$, $\mathscr{L}_{c_p\to\infty}\, \omega = \sqrt{\gamma}$ (cutoff frequency).

The qualitative behavior of the solution is illustrated in Fig. 2. The solution in Region II corresponds to the primary mode of propagation while that in Region IV is a secondary mode. The zero frequency limit of the primary mode, c_0, can be shown to agree identically

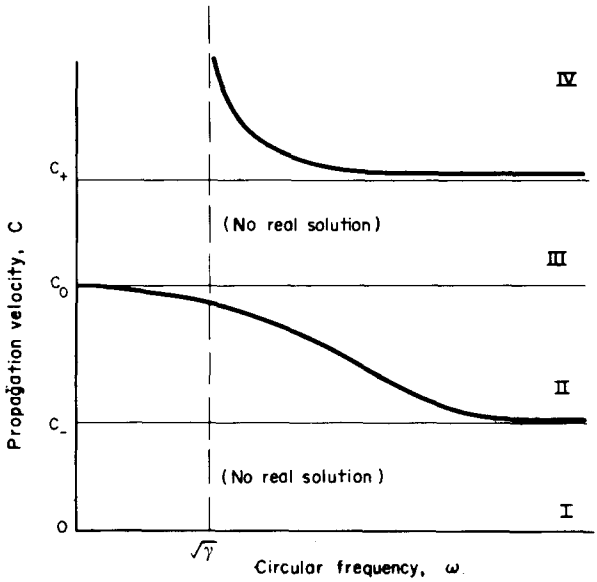

FIG. 2. Qualitative behavior of continuum mixture dispersion for laminates.

with the elasticity solution of Rytov [9]. This result is to be expected since the zero frequency limit corresponds to the static elastic solution, and the continuum relations were derived in such a way as to guarantee satisfaction of the static solution. The continuum model does, however, diverge increasingly from the exact solution with increasing frequency, becoming asymptotic to velocity c_- rather than the shear, or in some cases the Stoneley wave velocity predicted by elasticity theory [10].

Typical quantitative behavior of the first mode is illustrated in Figs. 3(a) and (b). Here the continuum model is compared with the exact elasticity solution derived by Rytov, and experimental data reported by Whittier and Peck [11] for Thornel or boron reinforced carbon phenolic laminates. Material properties for the two materials studied are given in Tables 1 and 2. As can be observed, agreement between exact and approximate theories is good for wavelengths greater than the typical composite microdimension. Fortunately, in cases involving sufficiently long input pulses it is the low-frequency components (wave lengths greater than the typical microdimension) which appear to dominate the overall character of a transient solution (see [12]).

A simplified continuum theory

Under certain boundary conditions (see following section) the foregoing continuum model can be simplified in a manner consistent with the premise that $\varepsilon \ll 1$. Consider, for example, (2.27). If we introduce the non-dimensional variables (2.18a) then (2.27) becomes

$$[(\partial_\xi^2 - \partial_t^2) + \varepsilon^2(A_1\partial_\xi^4 + A_2\partial_\xi^2\partial_t^2 + A_3\partial_t^4)]\Phi = 0, \tag{2.31}$$

where

$$A_1 \equiv (c_3^4 - c_1^2c_2^2)/\gamma c_0^2, \qquad A_2 \equiv (c_1^2 + c_2^2)/\gamma, \qquad A_3 \equiv -c_0^2/\gamma. \tag{2.32}$$

TABLE 1. THORNEL–CARBON PHENOLIC LAMINATE

	Thornel laminate	Carbon phenolic laminate
Density (g/cm^3)	1·47	1·42
Shear modulus, μ (dyn/cm^2)	7·56 (10^{11})	6·62 (10^{10})
Lamé constant, λ (dyn/cm^2)	7·56 (10^{11})	11·4 (10^{10})
Laminate thickness, $2h_\alpha$ (cm)	0·0064	0·0558
Volume fraction, n_α	0·104	0·896

TABLE 2. BORON–CARBON PHENOLIC LAMINATE

	Boron laminate	Carbon phenolic laminate
Density (g/cm^3)	2·37	1·42
Shear modulus, μ (dyn/cm^2)	9·51 (10^{11})	6·62 (10^{10})
Lamé constant, λ (dyn/cm^2)	8·06 (10^{11})	11·4 (10^{10})
Laminate thickness, $2h_\alpha$ (cm)	0·0104	0·0521
Volume fraction, n_α	0·166	0·834

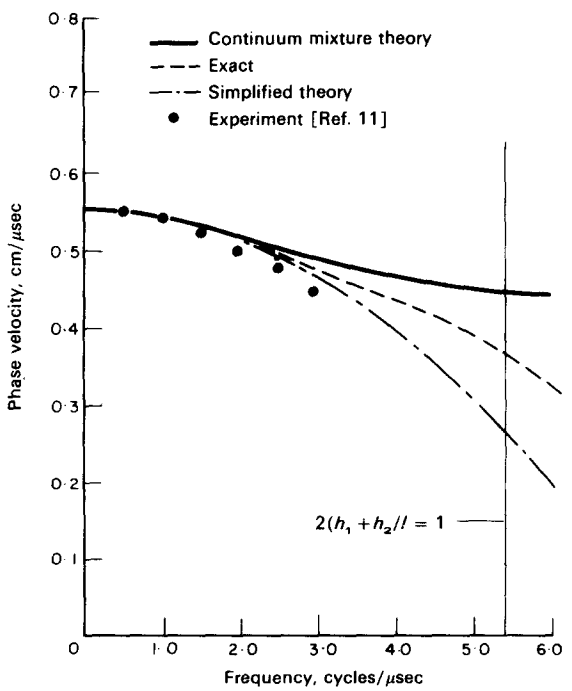

FIG. 3. (a) Phase velocity vs. frequency for Thornel reinforced carbon phenolic laminate.

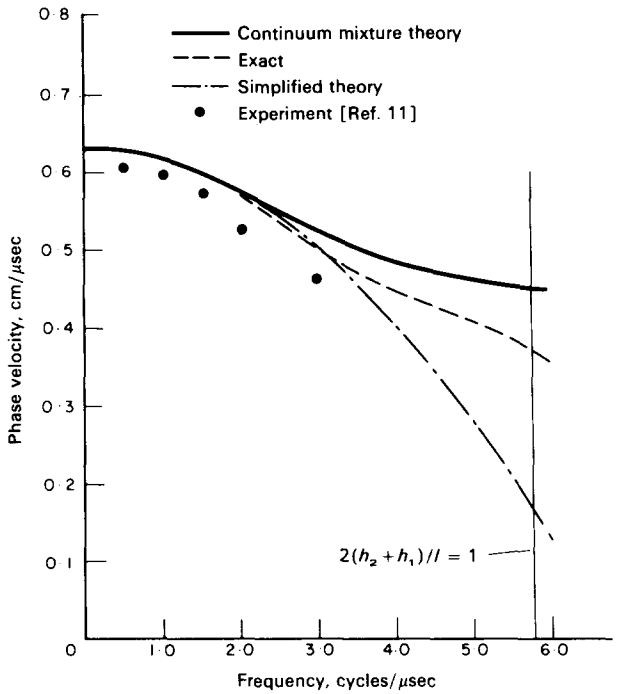

FIG. 3. (b) Phase velocity vs. frequency for boron reinforced carbon phenolic laminate.

Let us now expand Φ in the following regular asymptotic expansion:

$$\Phi(\xi, \tau; \varepsilon) = \Phi_0(\xi, \tau) + \varepsilon^2 \Phi_2(\xi, \tau) + \ldots . \tag{2.33}$$

Substituting (2.33) into (2.32) and equating orders of ε, we obtain

$$(\partial_\xi^2 - \partial_\tau^2)\Phi_0 = 0, \tag{2.34a}$$

$$(\partial_\xi^2 - \partial_\tau^2)\Phi_2 + [A_1\partial_\xi^4 + A_2\partial_\tau^2\partial_\xi^2 + A_3\partial_\tau^4]\Phi_0 = 0. \tag{2.34b}$$

The first of (2.34) implies that nondimensional space and time derivatives may be interchanged when operations are on Φ_0. Using this property, multiplying (2.34b) by ε^2 and adding the product to (2.34a) results in, to $O(\varepsilon^2)$ accuracy,

$$[(\partial_\xi^2 - \partial_\tau^2) + \varepsilon^2(A_1 + A_2 + A_3)\partial_\xi^2\partial_\tau^2](\Phi_0 + \varepsilon^2\Phi_2) = 0. \tag{2.35}$$

We note that a term of $O(\varepsilon^4)$ was added to (2.35); this, of course, does not alter the solution of $O(\varepsilon^2)$. Thus, to $O(\varepsilon^2)$ accuracy we obtain, in dimensional form,

$$[\partial_x^2 - c_0^{-2}(\partial_t^2 - \beta^{-2}\partial_x^2\partial_t^2)]\Phi = 0, \tag{2.36a}$$

where

$$\beta^{-2} \equiv \frac{c_3^4 - (c_0^2 - c_1^2)(c_0^2 - c_2^2)}{\gamma c_0^2}, \tag{2.36b}$$

Equation (2.36) is the well known Love–Rayleigh equation encountered in rod wave propagation problems. All dispersion information is contained in the coefficient β. We note that when both material properties are the same, β^{-2} vanishes and renders the medium nondispersive. The $c_p-\omega$ dispersion relation of (2.36) is parabolic in ω. A typical comparison of the spectra of (2.36), (2.27) and the exact elasticity solution is illustrated in Figs. 3(a), (b) for the laminates described in Tables 1 and 2.

Boundary conditions

To complete our formulation, we offer a few remarks concerning proper boundary conditions for the continuum and the simplified continuum theories.

For the continuum theory defined by (2.10), (2.20) and (2.26b), stresses $\overset{(\alpha p)}{\sigma}_{xx}$ ($\alpha = 1$ and 2) or displacements $\overset{(\alpha a)}{u}_x$ ($\alpha = 1$ and 2) may be prescribed along the boundaries $x = 0$, $x = L$, where $x \in [0, L]$. The displacement condition may be replaced by a velocity condition.

The situation is not as straightforward for the simplified continuum model (2.36) and care must be exercised when specifying boundary data. In contrast to the aforementioned original theory, here one cannot specify stresses or displacements in each constituent at a given boundary. It can be shown that the appropriate boundary condition for (2.36) when $\Phi \equiv \overset{(\alpha a)}{u}_x$ is $\overset{(\alpha a)}{u}_x = f(t)$ at $x = 0$, where $\alpha = 1$ and 2. In other words, the displacement field must be uniform with respect to y at $x = 0$. A similar statement applies to the boundary $x = L$. The stress field, consistent with the simplifications in the continuum model, may be computed from (2.20) with $\overset{(1a)}{u}_x \simeq \overset{(2a)}{u}_x$. In contrast to the displacements, the stress fields in the two constituents may be markedly different.

From (2.20) with $\overset{(1a)}{u}_x \simeq \overset{(2a)}{u}_x$, it can be seen that specification of the area-averaged stress $\overset{(s)}{\sigma}_{xx} = \overset{(1p)}{\sigma}_{xx} + \overset{(2p)}{\sigma}_{xx}$ is mathematically equivalent to the prescription of the boundary displacement. When the physical problem concerns stress boundary conditions (e.g. shock tube loading), it has been found that $\overset{(s)}{\sigma}_{xx}$ as a boundary condition yields adequate results once the wave has propagated beyond a few microdimensions from the given boundary†. It is evident that $\overset{(s)}{\sigma}_{xx}$ satisfies (2.36a).

Pulse propagation

The utility of the continuum models is perhaps best demonstrated by comparison of theoretical pulse propagation results with experimental data. To this end the momentum equations (2.10), interaction term (2.26b), and constitutive relations (2.20) were incorporated into a numerical finite difference code and the results of calculations were compared with the experimental data of Whittier and Peck [11]. Their specimens were composed of boron or Thornel layers reinforcing a carbon phenolic matrix. Specimens of $\frac{1}{4}$-in. thickness were subjected to a uniform pressure at the left boundary, with a step function time dependence induced by a gas dynamic shock wave of about 70 psi. Rear surface velocity, averaged across a $\frac{3}{8}$-in. dia. area of the specimen, was measured by means of a capacitance gage.

The calculations were begun by impacting a step function velocity of 7·786 cm/s to

† Mathematically, it can be shown that the original and simplified continuum theories yield similar results a distance $x = O(\sqrt{[l(h_1+h_2)]})$ from a given boundary.

both constituents at the boundary $x = 0$. While this condition did not correspond precisely to that of the experiment, which applied uniform stress at the boundary, it was felt that the error introduced would be negligible at the rear surface of the specimens.

Figures 4 and 5 depict the comparison between experimental and theoretical results for averaged rear surface velocity, normalized on the impact velocity $V_0 = 7{\cdot}786$ cm/s. The physical data on the composites is presented in Tables 1 and 2. Since absolute times were not measured in these tests, theoretical and experimental results were matched at their respective first peak arrivals. The times shown in the figures were those predicted by the continuum model.

The results on the Thornel composite agree somewhat better with the experiments than do those of the boron composite. As noted by Whittier and Peck, this may be due to the fact that the Thornel reinforcement more nearly approximates a homogeneous layer than does the boron. Considering the latter, as well as other differences between the laminated medium idealization and the actual test specimen, correlation is excellent, particularly at the head of the wave.

Finally, let us consider the more elementary theory (2.36). For a step of magnitude V_0 in velocity at the boundary $x = 0$ of a semi-infinite media occupying the space $x > 0$, the appropriate solution of the Love–Rayleigh equation is

$$\overset{(xa)}{\partial_t u_x} = V_0 - \frac{2V_0}{\pi}\int_0^b \cos \rho t \sin[\beta x\rho/\sqrt{(b^2-\rho^2)}]\,\mathrm{d}\rho/\rho, \tag{2.37}$$

where $b = c_0\beta$. For $V_0 = 7{\cdot}786$ cm/s, representing the steady state value of velocity, results obtained from (2.37) via a Gaussian quadrature routine are also compared with the original continuum model in Figs. 4 and 5. Based upon this comparison, it would appear that the simplified continuum theory yields adequate accuracy.

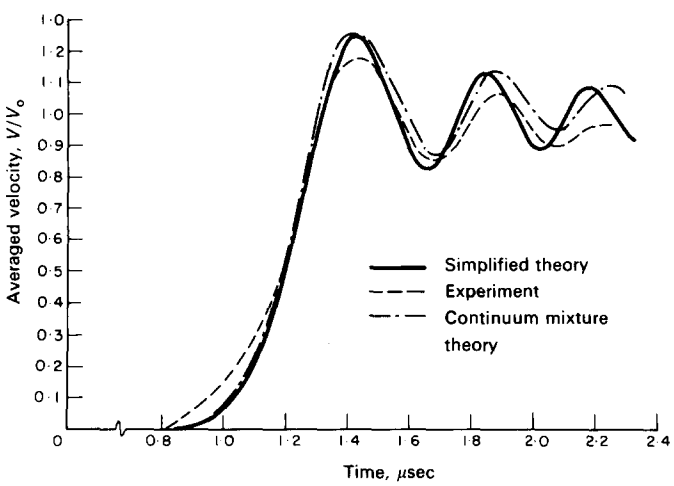

FIG. 4. Comparison of continuum mixture and simplified theories with experimental rear surface velocity results for Thornel reinforced carbon phenolic laminates.

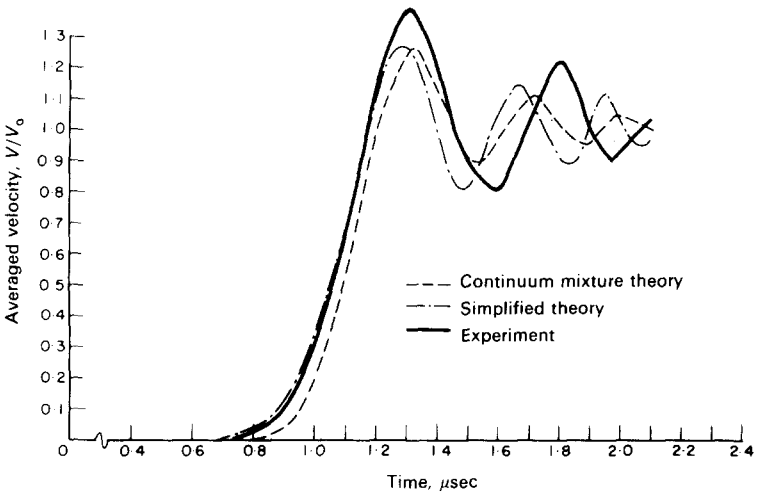

FIG. 5. Comparison of continuum mixture and simplified theories with experimental rear surface velocity results for boron reinforced carbon phenolic laminates.

3. ANALYSIS AND RESULTS FOR FIBROUS COMPOSITES

With minor modifications, the procedure outlined in previous sections can be applied to wave propagation parallel to the fibers of a uni-directionally reinforced composite with hexagonal array.

Formulation

We begin by approximating a hexagonal array by concentric, linearly elastic cylinders, with perfect interface bonds and subject to vanishing shear stress and radial displacement on the outer boundaries, as illustrated in Fig. 6. With respect to this approximation, the relevant equations are:

(i) Equation of motion:

$$\partial_x^{(\alpha)}\sigma_{xx} + \frac{1}{r}\partial_r^{(\alpha)}(r\sigma_{xr}) = \rho_\alpha \partial_t^2 u_x^{(\alpha)}, \tag{3.1}$$

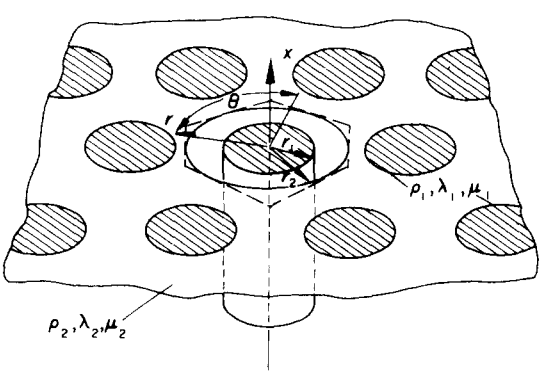

FIG. 6. Uni-directionally fiber-reinforced composite with hexagonal array.

(ii) Constitutive relations:

$$\overset{(\alpha)}{\sigma}_{xx} = \frac{\lambda_\alpha}{r}\partial_r(r\overset{(\alpha)}{u}_r) + (\lambda+2\mu)_\alpha \partial_x \overset{(\alpha)}{u}_x, \tag{3.2a}$$

$$\overset{(\alpha)}{\sigma}_{rr} = \lambda_\alpha\left(\frac{\overset{(\alpha)}{u}_r}{r} + \partial_x \overset{(\alpha)}{u}_x\right) + (\lambda+2\mu)_\alpha \partial_r \overset{(\alpha)}{u}_r, \tag{3.2b}$$

$$\overset{(\alpha)}{\sigma}_{rx} = \mu_\alpha(\partial_x \overset{(\alpha)}{u}_r + \partial_r \overset{(\alpha)}{u}_x). \tag{3.2c}$$

Here $\alpha = 1$ denotes fiber and $\alpha = 2$ denotes matrix.

(iii) Symmetry conditions:

$$\overset{(2)}{u}_r(x, r_2, t) = \overset{(2)}{\sigma}_{rx}(x, r_2, t) = 0, \tag{3.3}$$

(iv) Interface conditions:

$$\overset{(1)}{u}_r = \overset{(2)}{u}_r, \qquad \overset{(1)}{u}_x = \overset{(2)}{u}_x, \qquad \overset{(1)}{\sigma}_{rr} = \overset{(2)}{\sigma}_{rr}, \qquad \overset{(1)}{\sigma}_{rx} = \overset{(2)}{\sigma}_{rx} \tag{3.4}$$

on $r = r_1$.

(v) Appropriate initial data at time $t = 0$ and boundary conditions on $x = 0, L$, where $x \in [0, L]$.

Mixture equations of motion

If (3.1a) is multiplied by $2\pi r$, integrated from $r = 0$ to $r = r_1$ for $\alpha = 1$ and from $r = r_1$ to $r = r_2$ for $\alpha = 2$, and if continuity of shear stress across $r = r_1$ is invoked, the result can be written in the form (2.10) where, for this case,

$$\begin{aligned} P &\equiv \frac{2n_1}{r_1}\sigma_{rx}(x, r_1, t), \\ n_1 &\equiv r_1^2/r_2^2, \qquad n_2 \equiv (r_2^2 - r_1^2)/r_2^2, \\ \overset{(1a)}{(\ )} &\equiv \frac{1}{\pi r_1^2}\int_0^{r_1} (\ )^1 2\pi r\, dr, \\ \overset{(2a)}{(\ )} &\equiv \frac{1}{\pi(r_2^2 - r_1^2)}\int_{r_1}^{r_2} (\ )^2 2\pi r\, dr. \end{aligned} \tag{3.5}$$

Expansions and recurrence relations

For the present problem it is convenient to expand stresses and displacements in fiber and matrix in the form:

$$\overset{(\alpha)}{g}(x, r_\alpha^*, t) \equiv \overset{(\alpha)}{g}_{(0)}(x, t) + \overset{(\alpha)}{g}_{(1)}(x, t) r_\alpha^* + \ldots \overset{(\alpha)}{g}_{(n)}(x, t)\frac{r_\alpha^{*n}}{n!} + \ldots, \tag{3.6}$$

where

$$r_1^* \equiv r_1, \qquad r_2^* \equiv r_2 - r, \tag{3.7}$$

and $\overset{(1)}{g}$ denotes stress or displacement in the fiber while $\overset{(2)}{g}$ denotes same in the matrix.

Substitution of (3.6) into (3.1) and (3.2) yields a system of differential recurrence relations similar to (2.13) and (2.14). Since our objective here is the derivation of a first-order theory

only, we shall not list the complete set of such relations. Rather, the relevant equations will be noted in the course of the analysis.

Mixture constitutive relations

If (3.2a) is averaged according to (3.5), and continuity of $\overset{(\alpha)}{u}_r$ at $r = r_1$ is invoked, the result is

$$\begin{aligned} a_1\overset{(1p)}{\sigma}_{xx} - b_1 n_1 \partial_x \overset{(1a)}{u}_x &= u_r^*, \\ a_2\overset{(2p)}{\sigma}_{xx} - b_2 n_2 \partial_x \overset{(2a)}{u}_x &= -u_r^*, \end{aligned} \tag{3.8}$$

where

$$\begin{aligned} a_\alpha &\equiv 1/\lambda_\alpha, \qquad b_\alpha \equiv (\lambda_\alpha + 2\mu_\alpha)/\lambda_\alpha, \\ u_r^* &\equiv \frac{2n_1}{r_1}\overset{(1)}{u}_r(x, r_1, t). \end{aligned} \tag{3.9}$$

Using the first two terms in the expressions (3.6) together with a similar averaging of (3.2b) furnishes

$$\overset{(1a)}{\sigma}_{rr} = \frac{1}{a_1}\partial_x \overset{(1a)}{u}_x + \frac{d_1}{n_1}u_r^*, \tag{3.10}$$

$$\overset{(2a)}{\sigma}_{rr} = \frac{1}{a_2}\partial_x \overset{(2a)}{u}_x - \frac{1}{n_2}\left(d_2 + \mu_2\frac{r_2}{r_1}\right)u_r^*, \tag{3.11}$$

where

$$d_\alpha = (\lambda_\alpha + \mu_\alpha). \tag{3.12}$$

If $\overset{(\alpha a)}{\sigma}_{rr}$ are subjected to a condition similar to (2.18c), then solving for u_r^* between equations (3.10) and (3.11) we obtain

$$Eu_r^* = \frac{1}{a_2}\partial_x \overset{(2a)}{u}_x - \frac{1}{a_1}\partial_x \overset{(1a)}{u}_x, \tag{3.13a}$$

where

$$E \equiv \frac{1}{n_1 n_2}[(\lambda_1 + \mu_1)n_2 + (\lambda_2 + \mu_2)n_1 + \mu_2\sqrt{n_1}]. \tag{3.13b}$$

Finally, substituting (3.13a) into (3.8) we find the mixture constitutive equations satisfy (2.20) with $c_{\alpha\beta}$ redefined as

$$\begin{aligned} c_{\alpha\alpha} &= (\lambda_\alpha + 2\mu_\alpha)n_\alpha - \lambda_\alpha^2/E, \\ c_{\alpha\beta} &= \lambda_\alpha\lambda_\beta/E \qquad (\alpha \neq \beta). \end{aligned} \tag{3.14}$$

In contrast to the laminate analysis, the first few terms of the fiber expansion (3.6) do not contain the static elasticity solution. Consequently, the resultant modulus $c_{\alpha\alpha} + c_{\beta\beta} + 2c_{\alpha\beta}$ differs from the exact static composite modulus. The exact static modulus as given in [10] may be obtained by replacing the $\sqrt{n_1}$ in (3.13b) by unity.

Interaction term P

With the use of (3.6) equation (3.2c) for $\alpha = 1$ can be written

$$\overset{(1)}{\partial_r u_x} = \left(\frac{1}{\mu_1}\overset{(1)}{\sigma_{rx(1)}} - \overset{(1)}{\partial_x u_{r(1)}}\right) r + O(r^2). \tag{3.15}$$

If we multiply (3.15) by r, integrate by parts with respect to r from $r = 0$ to $r = r_1$, we obtain

$$\overset{(1)}{u_x}(x, r_1, t) - \overset{(1a)}{u_x} \simeq \frac{r_1^2}{2}\left(\frac{1}{\mu_1}\overset{(1)}{\sigma_{xr(1)}} - \overset{(1)}{\partial_x u_{r(1)}}\right). \tag{3.16}$$

Similarly for (3.2d) with $\alpha = 2$, we multiply by $(r^2 - r_1^2)/(r_2^2 - r_1^2)$, expand $\overset{(2)}{u_r}$ and $\overset{(2)}{\sigma_{rx}}$ in powers of $r_2^* = (r_2 - r)$ to $r_2^* = 0$, and integrate by parts to obtain

$$\overset{(2)}{u_x}(x, r_1, t) - \overset{(2a)}{u_x} \simeq \left(\frac{1}{\mu_2}\overset{(2)}{\sigma_{xr(1)}} - \overset{(2)}{\partial_x u_{r(1)}}\right) Q, \tag{3.17}$$

where

$$Q \equiv \frac{(r_2 - r_1)^3}{r_1 + r_2}\left(\frac{2}{3}\frac{r_2}{r_2 - r_1} - \frac{1}{4}\right). \tag{3.18}$$

Since $\overset{(1)}{u_x}(x, r_1, t) = \overset{(2)}{u_x}(x, r_1, t)$, equations (3.16) and (3.17) furnish

$$\overset{(1a)}{u_x} - \overset{(2a)}{u_x} = \left(\frac{Q}{\mu_2(r_1 - r_2)} - \frac{r_1}{4\mu_1}\right)\sigma_{rx}^* + \left(\frac{Q}{r_2 - r_1} + \frac{r_1}{4}\right)\partial_x u_r^*, \tag{3.19}$$

where

$$\sigma_{rx}^* \equiv \overset{(1)}{\sigma_{rx}}(x, r_1, t) = \overset{(2)}{\sigma_{rx}}(x, r_2, t).$$

However, from (3.13a), and following the discussion concerning the laminate interaction term, the last term in (3.19) can be shown to be of higher order than the first with respect to the parameter $\varepsilon = r_2/l$. The interaction term, therefore, takes the form (2.26b) with $K/(h_1 + h_2)^2$ replaced by K^*, where

$$K^* = \frac{8n_1\mu_1\mu_2}{r_1\left[\dfrac{4\mu_1 Q}{r_2 - r_1} + r_1\mu_2\right]}. \tag{3.20}$$

Phase velocity spectrum

The form of the fiber equations of motion and constitutive relations are identical to those of the laminates. The two differ only in the geometric dependence of their constants. Consequently, equations (2.27), (2.30) and (2.36) are applicable to the fiber geometry.

In Fig. 7, a comparison of the continuum model (first mode) dispersion relation is made with the exact elasticity solution derived by DeRuntz [10]. The properties elected are representative of a uni-directional fibrous quartz phenolic, the material and geometric properties of which are given in Table 3. Once again, agreement between the continuum and exact results is excellent for wavelengths greater than the microdimension of the composite, and progressively poorer as frequency increases.

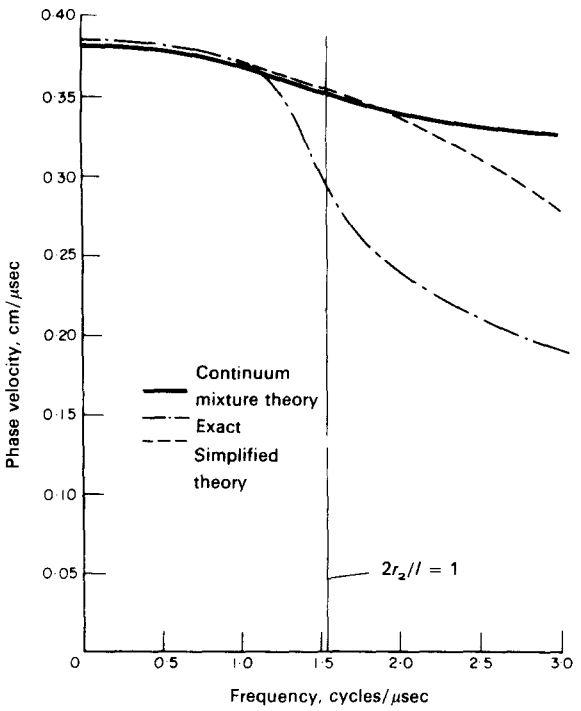

FIG. 7. Phase velocity vs. frequency for quartz fiber reinforced phenolic.

Simplified theory

The simplified theory (2.36) applies to the fiber geometry subject to the appropriate redefinitions of constants K^*, n_α, and $c_{\alpha\beta}$ ($\alpha, \beta = 1, 2$).

Pulse propagation

In Fig. 8, typical results of transient pulse data as predicted by the continuum theory is compared with experimental data on the uni-directional quartz phenolic fibrous composite described previously. The experiments were performed by the Aerospace Corporation. Specimens were subjected to a 70 psi step function in pressure via a shock tube. The experimental apparatus was identical to that described in [11]. Rear surface velocities, averaged across a $\frac{1}{2}$-in. dia. circle, were measured on a specimen 0·633 cm thick. Constituent data input was as given in Table 3. The figure depicts the comparison between the experimental and finite difference code predictions of area-averaged rear surface velocities. We again began our calculations by imparting an equal step function velocity to both

TABLE 3. QUARTZ FIBER REINFORCED PHENOLIC

	Quartz fiber	Phenolic
Density (g/cm^3)	1·85	1·29
Shear modulus, μ (dyn/cm^2)	106 (10^9)	30·3 (10^9)
Lamé constant, λ (dyn/cm^2)	327 (10^9)	75·8 (10^9)
Fiber radius, r_1 (cm)	0·0508	—
Outer matrix radius, r_2 (cm)	—	0·0975
Volume fractions, n_α	0·272	0·728

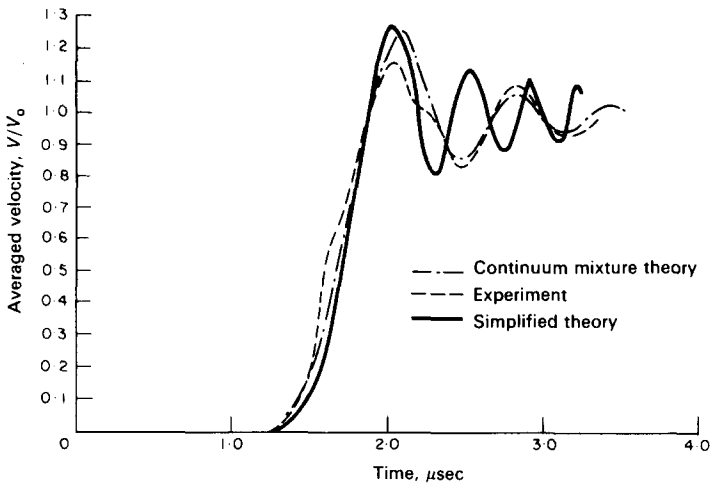

FIG. 8. Comparison of continuum mixture and simplified theories with experimental rear surface velocity results for quartz fiber reinforced phenolic.

constituents at $x = 0$. As was pointed out previously, the condition differs from that of uniform stress on the boundary, but is not expected to significantly influence the results at the rear surface of the test specimens. Results for our simplified theory (2.37) are also included in the figure for comparison.

Once again, absolute arrival times of the stress waves were not measured experimentally, and theoretical and experimental results were matched at approximately their first peak arrivals. The times shown in the figure correspond to those predicted by theory.

In this series of calculations, correlation between the simplified theory and the experimental data is considerably poorer than in both laminate tests. Agreement between the complete theory and the experiment is excellent however. A possible explanation of this might be found in studying the dispersion results for the quartz fiber reinforced phenolic (Fig. 7). First, the relatively large microdimensions of this composite causes the exact and continua theories to diverge at much lower frequencies than for the two laminates investigated. Further, the combination of quartz and phenolic material properties are such as to cause the parabolic dispersion curve predicted by the simplified theory to diverge significantly from the continuum and exact theories, at even low frequencies. A parametric study was performed on both material and geometric constituent properties for the fiber case, and it was found that for dimensions and material property data similar to those of the laminates investigated (Tables 1 and 2), correlation between continuum, simplified and exact predictions of dispersion in the fiber case could be enhanced considerably.

It should be noted that the fibers used in the quartz phenolic are actually bundles of approximately 11,500 individual quartz filaments woven into a yarn with a phenolic binder. Thus, as might be expected, the fibers were found to possess highly anisotropic material properties. We have, however, modeled the fiber bundle material as isotropic using the material properties in the longitudinal fiber direction in our calculations.

Concluding remarks

A continuum theory was constructed for wave propagation in laminated and fibrous composites for the case of waves traveling in the direction of reinforcements. The theory is

given in a binary mixture form by (2.10), (2.20) and (2.26). A simplified theory, valid for certain boundary conditions, is given by (2.36). Once the dependent variables of the theory are known (partial stresses and average displacements), the approximate microstructure (stress and displacement distributions within each constituent) may be constructed up to linear or quadratic dependence on the spatial coordinate transverse to the direction of propagation.

A comparison of exact and approximate phase velocity data (see Fig. 3(a), (b) for laminates, Fig. 7 for fibers) indicates that the theory provides good first mode agreement for wavelengths greater than the typical composite microdimension. In addition, experimental transient pulse data on boron–carbon phenolic and Thornel–carbon phenolic laminates, as well as a quartz phenolic fibrous composite, correlates well with the continuum theory results. Hence, we conclude the model is a practical one, particularly in view of its simplicity.

Finally, if additional accuracy is deemed necessary, additional terms in all expansions may be retained. While a similar construction procedure as used here can be followed, the resulting theory will be considerably more complex than the present one. As such, its practical utility may be limited.

Acknowledgements—The research reported herein was sponsored by the Air Force Weapons Laboratory under Contract No. F29601-71-C-0030. The authors are indebted to Mr. E. W. Sims for his considerable efforts in performing the necessary computations.

REFERENCES

[1] G. W. POSTMA, Wave propagation in a stratified medium. *Geophysics* **20**, 780 (1965).
[2] J. E. WHITE and F. A. ANGONA, Elastic wave velocities in laminated media. *J. acoust. Soc. Am.* **27**, 311 (1955).
[3] G. HERRMANN and J. D. ACHENBACH, On Dynamic Theories of Fiber Reinforced Composites, *Proc. AIAA/ASME Eighth Structl. Dynm. Mat. Conf.*, 112. Palm Springs, California (1967).
[4] C. T. SUN, J. D. ACHENBACH and G. HERRMANN, Continuum theory for a laminated medium. *J. Appl. Mech.* **35**, 467 (1968).
[5] J. D. ACHENBACH, C. T. SUN and G. HERRMANN, On the vibrations of a laminated body. *J. Appl. Mech.* **35**, 689 (1968).
[6] B. LEMPRIERE, On the Practicability of Analyzing Waves in Composites by the Theory of Mixtures, Lockheed Palo Alto Research Laboratory, Report No. LMSC-6-78-69-21 (1969).
[7] A. BEDFORD and M. STERN, Toward a diffusing continuum theory of composite materials. *J. appl. Mech.* **38**, 8 (1971).
[8] G. A. HEGEMIER, On a Theory of Interacting Continua for Wave Propagation in Composites, *Proc. Symp. Dynam. Comp. Mat.* La Jolla, California (1972).
[9] S. M. RYTOV, Acoustical properties of a thinly laminated medium, *Sov. Phys. Acoust.* **2**, 68 (1956).
[10] O. HOFFMAN, J. A. DERUNTZ, D. T. LIU, A. R. HUNTER and E. L. KYSER, Study of Advanced Filament-Reinforced Materials, Lockheed Missiles and Space Company, Report No. LMSC-N-5M-70-2 (1970).
[11] J. S. WHITTIER and J. C. PECK, Experiments on dispersive pulse propagation in laminated composites and comparisons with theory, *J. appl. Mech.* **36**, 485 (1969).
[12] J. C. PECK and G. A. GURTMAN, Dispersive pulse propagation parallel to the interfaces of a laminated composite. *J. appl. Mech.* **36**, 479 (1969).

(*Received* 16 *May* 1972; *revised* 23 *June* 1972)

Абстракт—Разрабатывается теория двойной смеси для распространения волн, направленного типа, в слоистих и ненаправленных волокнистых составах. В частности, дается построение взаимодействия двух смесей, и также, конститутивные зависимости. Получающаяся, в результате, теория содержит в себе микроструктуру.

Определяется область важности теории смеси, путем сравнения спектра фазовой скоротси с точным и, лиоо, или экспериментальным результатом. Указывается полезность модели, как для сложных так и волокнистых составов, на основе корреляции теоретических и экспериментальных данных, касающихся импульсного переходного процесса в составах типа бор—углеродная фенольная пластмасса и Торнел—углеродная фенольная пластмасса, или в однонаправленной, волокнистой, кварцевой фенольной пластмассе.